ChemPubSoc Europe

DOI: 10.1002/cplu.201600051

CHEMPLUSCHEM Full Papers

Dendrimeric Sulfanyl Porphyrazines: Synthesis, Physico-Chemical Characterization, and Biological Activity for Potential Applications in Photodynamic Therapy

Dariusz T. Mlynarczyk,[a] Sebastian Lijewski,[a] Michal Falkowski,[a] Jaroslaw Piskorz,[b] Wojciech Szczolko,[a] Lukasz Sobotta,[b] Magdalena Stolarska,[a, c] Lukasz Popenda,[d] Stefan Jurga,[d, e] Krystyna Konopka,[f] Nejat Düzgüneş,[f] Jadwiga Mielcarek,[b] and Tomasz Goslinski*[a]

Sulfanyl porphyrazines substituted at their periphery with different dendrimeric moieties up to their first generation were synthesized and characterized by photochemical and biological methods. The presence of a dendrimeric periphery enhanced the spectral properties of the porphyrazines studied. The singlet-oxygen-generation quantum yield of the obtained macrocycles ranged from 0.02 to 0.20 and was strongly dependent on the symmetry of the compounds and the terminal groups of the dendritic outer shell. The in vitro biological effects of three most promising tribenzoporphyrazines were examined; the results indicated their potential as photosensitizers for photodynamic therapy (PDT) against two oral squamous cell carcinoma cell lines derived from the tongue. The highest photocytotoxicity was found for sulfanyl tribenzoporphyrazine that possessed 4-[3,5-di(hydroxymethyl)phenoxy]butyl substituents with nanomolar IC_{50} values at 10 and 42 nM against CAL 27 and HSC-3 cell lines, respectively.

Introduction

Porphyrazines (Pzs) are macrocyclic compounds that consist of four pyrrole units linked together with azamethine groups in place of methine bridges present in porphyrins.[1] The spectroscopic, photochemical, and electrochemical properties of Pzs have been studied widely. These properties render them suitable for potential applications in photodynamic therapy (PDT) and photodynamic diagnosis (PDD) as photosensitizers, in chemical catalysis, and in analytical chemistry as sensors.[2–5] Porphyrazines that contain sulfanyl substituents reveal good solubility in common organic solvents and significant photocytotoxicities.[6–9] Many years of research on sulfanyl porphyrazines led to the expansion of their periphery with various groups; for example, ether/thioether,[10,11] calixarene,[12] (tetrathiafulvalene)sulfanylethyl,[13] 2′-(4-pyridoxy)ethyl,[14] 1-naphthylmethyl,[8] 2′-(ferrocenecarboxy)ethyl,[15] and 4-(4-nitroimidazol-1-yl)butyl.[16]

The possibility to add and modify dendrimer substituents at the periphery of macrocyclic rings has been applied so far for porphyrins and phthalocyanines.[17,18] It has been shown that dendrimeric moieties around the porphyrinoid core significantly affect their photophysical characteristics.[19] Dendrimers by themselves are highly branched polymers with unique physico-chemical and biological properties.[20,21] They have been considered drug-delivery systems because of their ability to transport various molecules within the structure of their dendrons. So far, dendrimers have been tested to be successful carriers of anticancer drugs (e.g., paclitaxel, doxorubicin), gadolinium compounds for diagnostic purposes, poorly water-soluble antimicrobials, and many others.[22] Dendrimers have also been investigated for PDT purposes.[21] The combination of phthalocyanines with dendrimer substituents enabled the extension of the possible biological applications of porphyri-

[a] D. T. Mlynarczyk, S. Lijewski, M. Falkowski, Dr. W. Szczolko, M. Stolarska, Dr. T. Goslinski
Department of Chemical Technology of Drugs
Poznan University of Medical Sciences
Grunwaldzka 6, 60-780 Poznan (Poland)
E-mail: tomasz.goslinski@ump.edu.pl

[b] Dr. J. Piskorz, Dr. L. Sobotta, Dr. J. Mielcarek
Department of Inorganic and Analytical Chemistry
Poznan University of Medical Sciences
Grunwaldzka 6, 60-780 Poznan (Poland)

[c] M. Stolarska
Department of Pharmaceutical Technology
Poznan University of Medical Sciences
Grunwaldzka 6, 61-780 Poznan (Poland)

[d] Dr. L. Popenda, Prof. Dr. S. Jurga
NanoBioMedical Centre
Adam Mickiewicz University in Poznan
Umultowska 85, 61-614 Poznan (Poland)

[e] Prof. Dr. S. Jurga
Faculty of Physics
Adam Mickiewicz University in Poznan
Umultowska 85, 61-614 Poznan (Poland)

[f] Prof. Dr. K. Konopka, Prof. Dr. N. Düzgüneş
Department of Biomedical Sciences
University of the Pacific
155 Fifth Street, San Francisco, CA 94103 (USA)

Supporting information and the ORCID identification number(s) for the author(s) of this article can be found under http://dx.doi.org/10.1002/cplu.201600051.

noids, reduced aggregation, and therefore increased the efficiency of singlet oxygen generation.[23] Dendrimers have also revealed a potential to catalyze chemical reactions enantioselectively. The bulky periphery of metalloporphyrinoids has been found to mimic enzymes, and these molecules have been applied in biomimetics.[24]

Herein, we report the synthesis of a series of dendrimer-substituted sulfanyl porphyrazines. They were obtained as a part of our research on sulfanyl porphyrazines that bear isophthaloxybutyl substituents on their periphery.[25,26] The novel compounds were characterized in terms of their photophysical properties. Selected sulfanyl tribenzoporphyrazines were subjected to photocytotoxicity studies.

Results and Discussion

Synthesis and characterization

The alkylation reaction of dimercaptomaleonitrile disodium salt **1** with 3,5-bis(3,5-dimethoxybenzyloxy)benzyl bromide **2** in dimethylformamide and with potassium carbonate as a base led to the novel maleonitrile derivative **3**. After its purification and thorough characterization, **3** was utilized in the Linstead macrocyclization reaction in *n*-butanol and in the presence of magnesium *n*-butanolate as a base to form the novel porphyrazine **4** (Scheme 1).[27]

3,5-Bis[3,5-bis(methoxycarbonyl)phenoxymethyl]phenol (**5**) was synthesized according to the Höger procedure.[28] Briefly, the hydroxyl group of a commercially available dimethyl 3-hydroxyisophtalate was protected in the reaction with silyl chloride. Next, ester groups were reduced to alcohol groups with lithium aluminum hydride. The obtained diol was subjected to the Mitsunobu reaction with dimethyl 5-hydroxyisophtalate to form a branched ether, the terminal aromatic hydroxyl group of which was deprotected using tetrabutylammonium fluoride to give **5**. The alkylation reaction of **5** with 1,4-dibromobutane in dimethylformamide and in the presence of potassium carbonate led to the derivative **6**, which was applied as the alkylating agent in the next step (Scheme 2). The alkylation reaction of dimercaptomaleonitrile disodium salt **1** with **6** in dimethylformamide and in the presence of potassium carbonate led to the novel maleonitrile derivative **7**. This compound was used subsequently in the Linstead macrocyclization reaction in *n*-butanol in the presence of magnesium *n*-butanolate to result in the symmetrical porphyrazine derivative **8**.[27] In another approach, **7** and 1,2-dicyanobenzene were used in the mixed Linstead macrocyclization reaction with Hoffman–Barrett modification in *n*-butanol and in the presence of magnesium *n*-butanolate, thus leading to the novel tribenzoporphyrazine derivative **9**.[29]

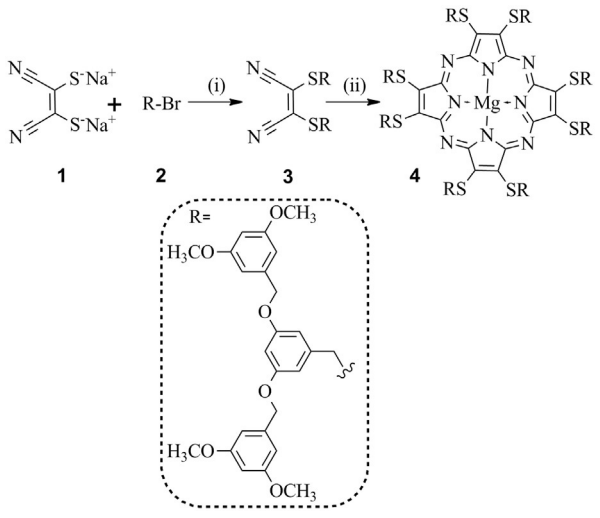

Scheme 1. Synthesis of compounds **3** and **4**. Reagents and conditions: (i) K_2CO_3, DMF, room temperature, 48 h; (ii) $Mg(nOC_4H_9)_2$, *n*BuOH, reflux, 20 h.

2,3-Bis[4-(3,5-dimethoxycarbonylphenoxy)butylsulfanyl]maleonitrile (**10**) was synthesized according to previously published procedures.[25,30] Briefly, the alkylation reaction of dimercaptomaleonitrile disodium salt with dimethyl 5-(4-bromobutoxy)isophthalate led to **10**. The tribenzoporphyrazine derivative **11** was obtained by means of the mixed Linstead macrocyclization reaction with the Hoffman–Barrett modification using **10** and 1,2-dicyanobenzene in *n*-butanol in the presence of magnesium *n*-butanolate (Scheme 3). The subsequent reduction reaction of **11** with lithium aluminium hydride was carried out using the procedure reported earlier by Höger[28] and led to the formation of the porphyrazine derivative **12**. The alkylation reaction of **12** was used in the divergent synthetic approach, which led to a tribenzoporphyrazine with G_1 dendrimeric moieties (**13**).

The novel sulfanyl porphyrazine derivatives were characterized using various methods, including UV/Vis, NMR, and mass spectrometry. HPLC analysis performed in three different solvent systems confirmed the purity of the macrocycles. NMR spectroscopy—and the ^1H–^{13}C HMBC technique in particular—was useful in elucidating the structure of **4**. The presence of correlation signals between C1, C4 pyrrole carbons at $\delta =$ 158.5 ppm and C2, C3 pyrrole carbons at $\delta = 141.7$ ppm with protons at $\delta = 5.72$ ppm allowed us to assign the SCH_2 hydrogen atoms. Other correlations observed between the outer peripheral C3″, C5″ benzyl carbons at $\delta = 161.9$ ppm to protons of the methoxy substituent at $\delta = 3.68$ ppm enabled us to distinguish between benzyl moieties of the outer and inner sphere within the dendrimeric substituents. There were no cross-peaks detected in the ^1H–^1H COSY spectrum of **4**, unlike in the ^1H–^1H COSY spectrum of **8**, in which correlations in both peripheral and linker groups were observed. That enabled the assignment of the signals of aliphatic protons of **8** present in the ^1H NMR spectra. In addition, cross-peaks between C2″ and C4″ of the outer sphere benzene rings were observed in **8**. Correlations observed in the ^1H–^{13}C HMBC between the butyl chain protons of terminal esters and C3″ aromatic carbons of the outer dendrimeric sphere permitted differentiation between the outer and inner benzene substituents.

In the ^1H–^1H COSY spectrum of tribenzoporphyrazine **11**, correlations within aliphatic protons were found (two groups of neighboring hydrogen atoms at $\delta = 3.85$, 1.35, 1.16, 0.74 ppm and $\delta = 4.32$, 3.75 1.97 ppm). The ^1H–^{13}C HMBC and ^1H–^{13}C HSQC spectra were required to assign the aromatic pro-

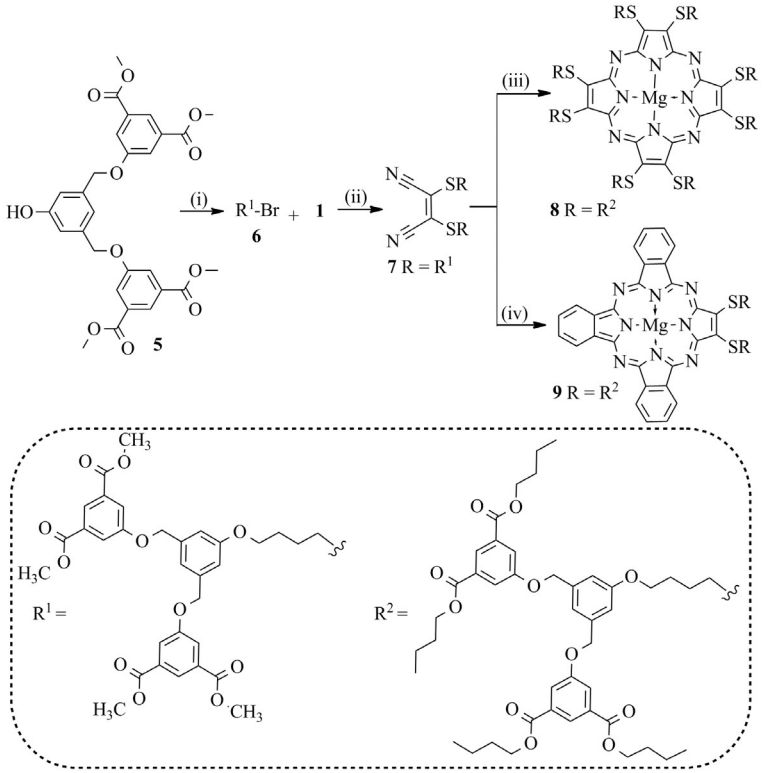

Scheme 2. Synthesis of compounds **6**–**9**. Reagents and conditions: (i) $Br(CH_2)_4Br$, K_2CO_3, DMF, 50 °C, 22 h; (ii) K_2CO_3, DMF, 50 °C, 21 h; (iii) $Mg(nOC_4H_9)_2$, *n*BuOH, reflux, 22 h; (iv) 1,2-dicyanobenzene, $Mg(nOC_4H_9)_2$, *n*BuOH, reflux, 20 h.

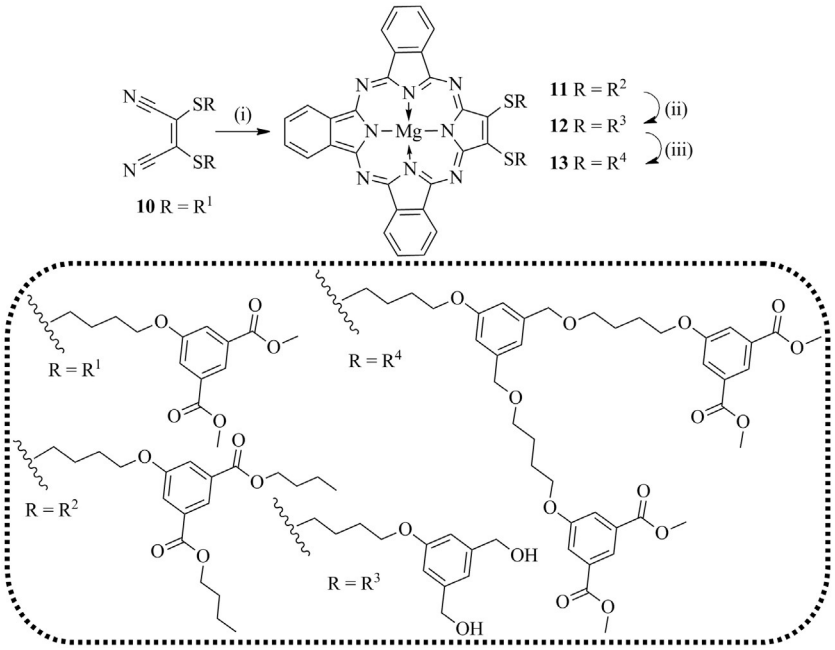

Scheme 3. Synthesis of compounds **11**–**13**. Reagents and conditions: (i) 1,2-dicyanobenzene, $Mg(nOC_4H_9)_2$, *n*BuOH, reflux, 20 h; (ii) $LiAlH_4$, THF; (iii) dimethyl 5-(4-bromobutoxy)benzene-1,3-dicarboxylate, Cs_2CO_3, DMF, 60 °C, 19 h. THF = tetrahydrofuran.

tons and carbon nuclei of isophthalate moieties present in the periphery. These spectra showed that peaks at $\delta = 4.32$ and 3.75 ppm correspond to OCH_2 and SCH_2 protons within the butyl linker, respectively. Proton peaks of the tribenzo part appeared in the range between $\delta = 8.10$–9.29 ppm as a group of peaks, which was also the case for other investigated tribenzoporphyrazines.[31]

Aliphatic protons and carbons in porphyrazine **12** were assigned using ^1H–^1H COSY and ^1H–^{13}C HSQC spectra. However, with the use of 2D techniques it was not possible to identify

protons and carbons of isophthalate and tribenzo fragments. Similar problems were found in **13** because of the overlapping peaks of aliphatic protons. For tribenzoporphyrazines **9** and **13**, both substituted with G_1-dendrimeric moieties, no correlations in the ^1H–^1H COSY and ^1H–^{13}C HMBC spectra between isophthalate and aliphatic moieties were observed. It hampered the possibility of assigning the signals that belonged to the inner and outer sphere of the dendrons.

Spectroscopic and singlet oxygen generation studies

The UV/Vis spectra of investigated porphyrazines show both a short-wavelength Soret band between 290–420 nm and a long-wavelength Q band between 550–750 nm. The first one is a result of π–π^* transitions from the molecular orbital (MO) to the lowest unoccupied molecular orbital (LUMO). The second band is also a consequence of π–π^* transitions, but in this case electrons are transferred from the highest occupied molecular orbital (HOMO) to LUMO. The LUMO orbital is degenerate or non-degenerate. Degeneration of the LUMO orbital depends on molecular symmetry.[32–34] In symmetrical porphyrazines this orbital is degenerate, and, as a consequence, in the UV/Vis spectrum a sharp unsplit Q band appears, which was the case for Pzs **4** and **8** (Figure 1). For tribenzoporphyrazines **9** and **13**, which are molecules of low symmetry, the situation was quite different. Their non-degenerate LUMO orbitals manifested themselves as a split band in the long-wavelength UV/Vis region. As shown in the study by Leclaire et al.,[19] the presence of bulky dendritic substituents in the periphery of a macrocycle is responsible for shielding the tetrapyrrolic core and thus for an increase in the Q-band intensity with every dendrimer generation added. In our study, the relative absorbance of the Q band of tribenzoporphyrazines **9** and **13** with G_0 and G_1 dendrimeric substituents of different size did not change significantly. However, important changes were observed during the photochemical study discussed below.

The novel porphyrazines were subjected to photochemical studies. Evaluation of singlet oxygen generation for the examined compounds was performed in DMF (*N*,*N*-dimethylformamide) according to the methodology described previously.[35–40] 1,3-Diphenylisobenzofuran (DPBF) was used as a singlet oxygen chemical quencher, whereas unsubstituted zinc phthalocyanine (ZnPc) with a known singlet oxygen quantum yield (0.56 and 0.67 in DMF and DMSO (dimethyl sulfoxide), respectively) was used as a reference. Mixtures of DPBF and porphyrazines **4**, **8**, **9**, and **11**–**13** were irradiated with light of an appropriate wavelength and changes in the UV/Vis spectra were studied (Figure 2a). DPBF, which is a known singlet oxygen trapping agent, was converted during the experiment to a very unstable endoperoxide according to the first-order kinetic model (Figure 2b); this manifested in the UV/Vis spectra as a decrease in the intensity of the band at 417 nm. The Pzs studied have low or moderate singlet-oxygen-generation efficacy, with the values reaching one half of that observed for unsubstituted zinc phthalocyanine (Table 1). For tribenzoporphyrazines, this might be the result of the decrease in symmetry.

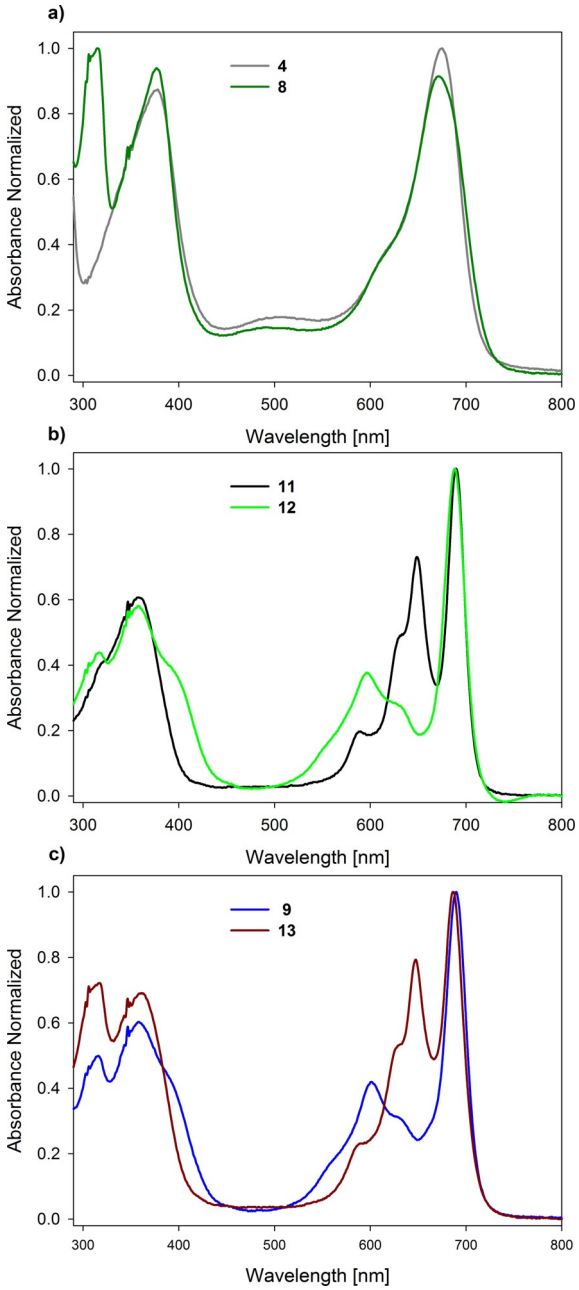

Figure 1. UV/Vis spectra of investigated compounds in DMF: (a) symmetrical porphyrazines **4** and **8**; (b) tribenzoporphyrazines **11** and **12**; and (c) tribenzoporphyrazines **9** and **13**.

Table 1. Quantum yields of singlet-oxygen generation by Pzs **4**, **8**, **9**, and **11**–**13** in DMF.

Pzs	Singlet-oxygen generation	
	Irradiation wavelength [nm]	Singlet-oxygen quantum yield [Φ_Δ][a]
4	674	0.03
8	672	0.02
9	690	0.15
11	690	0.05
12	688	0.20
13	686	0.09

[a] Error $\leq$ 0.01.

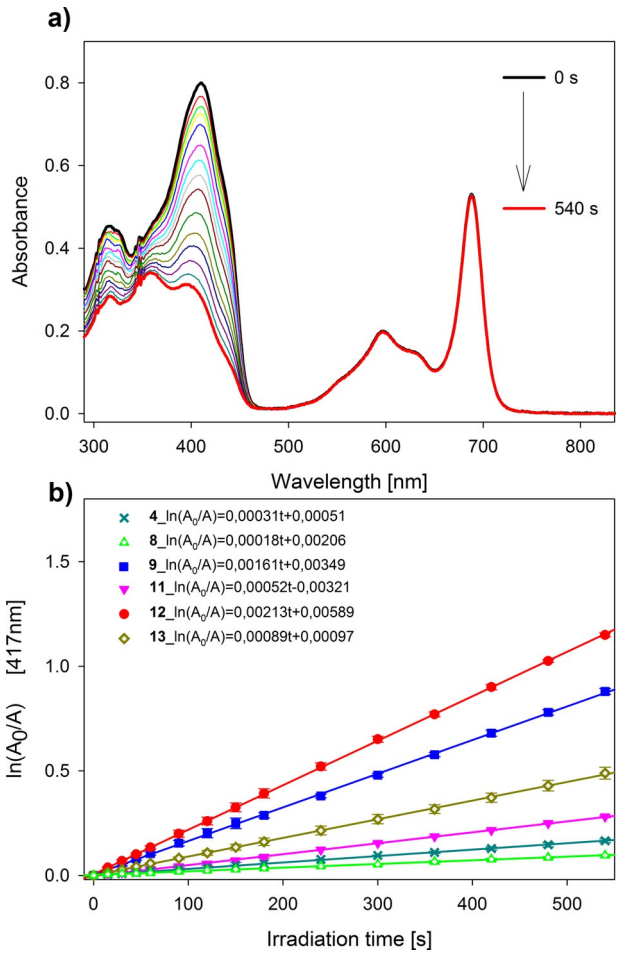

Figure 2. (a) Changes in the UV/Vis spectrum during irradiation of **12** and the DPBF mixture in DMF. (b) First-order plots for the oxidation of DPBF by photosensitized compounds **4**, **8**, **9**, and **11**–**13** in DMF.

Tribenzoporphyrazine derivative **12**, which is an analogue (hydroxyl groups at the periphery instead of carboxy) of **11**, shows the highest ability to generate singlet oxygen (Φ_Δ = 0.20) in DMF. The enlargement of the tribenzoporphyrazine periphery from G_0 to G_1 resulted in higher Φ_Δ values. The yield of singlet-oxygen generation increased three times from 0.05 for **11** to 0.15 for **9**, which is consistent with the literature data.[23] In **9** and **13**, both tribenzoporphyrazines with G_1 peripheral substituents, singlet-oxygen-generation values were 0.09 and 0.15, respectively. This can be the result of the distance between the inner and outer sphere within dendrimeric substituents. For octakis-substituted Pzs **4** and **8**, the singlet-oxygen-generation efficacy was relatively low (Φ_Δ = 0.03 for **4** and Φ_Δ = 0.02 for **8**). No increase in singlet-oxygen-generation efficacy was observed by enlargement of our recently published G_0 symmetrical porphyrazine[25] to **8**, as both revealed low singlet-oxygen-generation efficacies with yields of 0.02 in DMF. The photochemical data obtained for Pzs **4** and **8** comply with those previously published for sulfanyl Pzs.[25,41]

In vitro photocytotoxicity of selected tribenzoporphyrazines

The photodynamic activity of Pzs **9**, **11**, and **12** was investigated in vitro using two oral squamous cell carcinoma cell lines derived from the tongue (CAL 27, HSC-3). The dark toxicity of Pzs **9**, **11**, and **12** was evaluated at the limited concentration range of 0.1 to 10 μM. There was no significant dark toxicity observed for all compounds tested on both CAL 27 and HSC-3 cell lines (Figure 3). Therefore, the light-induced toxicity was examined at the same concentrations of Pzs as that used for dark toxicity measurements (0.1, 1.0, 10.0 μM) (Figure 3, Tables S11 and S12 in the Supporting Information).

All the compounds at 10.0 μM reduced the viability of both cell lines. Porphyrazine **11** at this concentration decreased the viability of CAL 27 cells by 58% and HSC-3 by 51%. Pz **9** reduced the viability of CAL 27 cells by 84% and HSC-3 cells by 95%, whereas Pz **12** showed photocytotoxicities higher than 90% against both cell lines.

In addition, Pz **9** and **12** had cytotoxic effects at 1.0 μM. Pz **9** decreased CAL 27 cell viability by 24% and HSC-3 by 69%. The highest reduction of CAL 27 and HSC-3 cell viabilities (above 95%) at 1.0 μM was obtained with Pz **12**. Moreover, Pz **12** at the lowest concentration used (0.1 μM) reduced the viability of CAL 27 cells by 99% and of HSC-3 cells by 95% (Figure 3, Table S11 and S12 in Supporting Information).

Further experiments with Pzs **9**, **11**, and **12** were performed at six concentrations for each compound to evaluate the correlation between the viability of the cancer cells and the concentration of photosensitizers (Figure 4, Tables S13 and S14 in the Supporting Information). Pz **9** and **11** were tested in the concentration range 0.1 to 10.0 μM, and Pz **12** was tested in the range of 0.005–1.0 μM. Calculation of the IC_{50} values indicated that Pz **12** had the highest photocytotoxicity with values of 10 nM for CAL 27 cells and 42 nM for HSC-3 cells.

In our previous in vitro photodynamic studies with oral squamous cell carcinoma (OSCC) cell lines, other porphyrinoid photosensitizers were investigated. The photosensitizing activity of two porphyrazines that possessed fluoroalkylthio and dietherthio substituents was examined using HSC-3 and H413 cells.[41] The fluorinated macrocycle showed about 30–35% photocytotoxicity on H413 cells at both 1.0 and 5.0 μM. However, there was no significant photosensitizing activity on HSC-3 cells. In another study, zinc phthalocyanine and its analogue with ester-alkyloxy substituents were tested against HSC-3 cells.[42] Zinc phthalocyanine decreased cell viability by 30% at 0.1 μM and by 100% at 5.0 μM. The photodynamic activity of the substituted phthalocyanine was significantly lower, with only 15% reduction of the viability of HSC-3 cells at 5.0 μM. Further experiments performed with magnesium(II) and zinc(II) phthalocyanines equipped with polyether substituents, and the magnesium(II) phthalocyanine–metronidazole conjugate revealed high in vitro photodynamic activity against HSC-3 cells.[43] All three phthalocyanine derivatives caused 100% photocytotoxicity at 5.0 μM. Moreover, zinc(II) phthalocyanine and the magnesium(II) phthalocyanine–metronidazole conjugate decreased the viability of HSC-3 cells at 0.1 μM by 17 and 34%, respectively. The photosensitizing activity toward HSC-3 cells

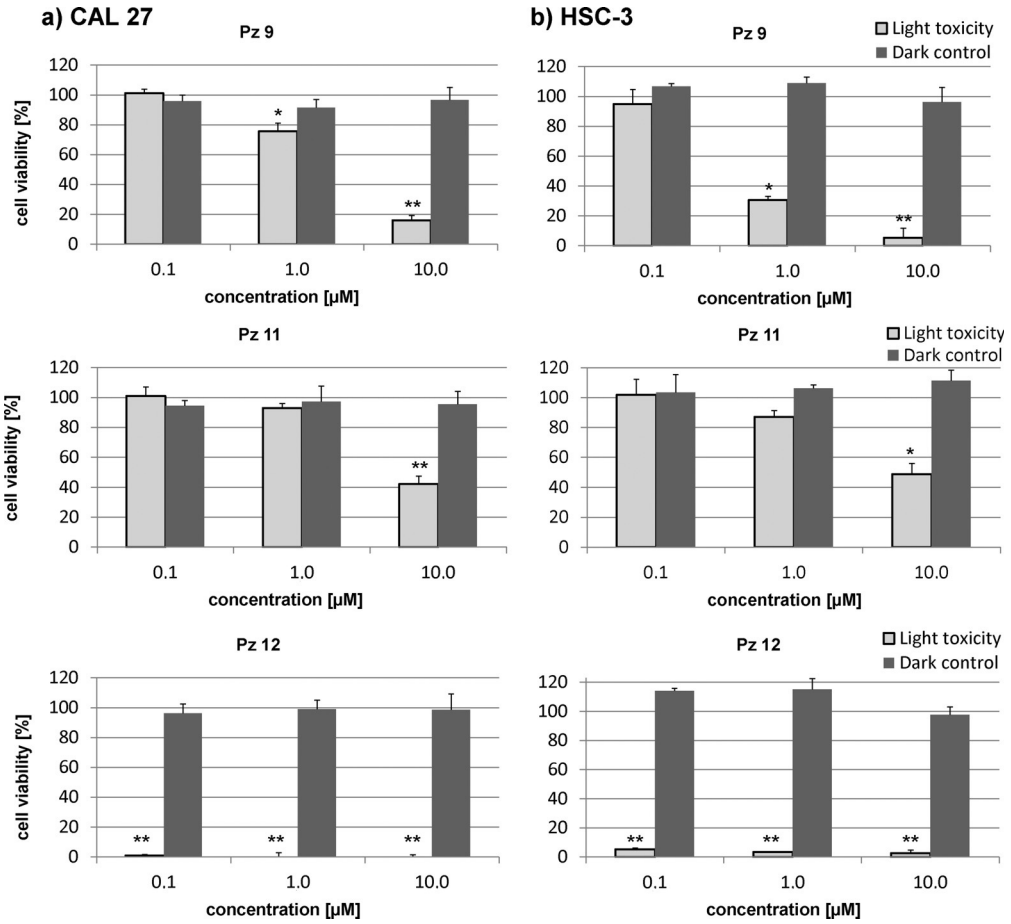

Figure 3. Light toxicity under 690 nm light irradiation (and dark control) of Pzs **9**, **11**, and **12** against: (a) CAL 27 and (b) HSC-3 cell lines. Data represent the mean ± standard deviation obtained from two independent experiments performed in triplicate. Statistical significance is indicated with asterisks: $*p < 0.001$, $**p < 0.0001$.

of demetalled porphyrazine and magnesium(II) tribenzoporphyrazine that possessed a diazepine substituent was demonstrated in another study.[2] Magnesium(II) tribenzoporphyrazine reduced cell viability by 95% at 1.0 μM and by about 50% at 0.1 μM. Demetalled porphyrazine showed 87% photocytotoxicity at 10.0 μM, but at 1.0 μM the viability of HSC-3 cells was unaffected. In addition, tribenzoporphyrazine had a photocytotoxic effect on H413 cells at 0.025 and 1.0 μM. These data demonstrate that Pz **12** exhibits the strongest photocytotoxicity against oral cancer cells of all the porphyrinoids synthesized so far by our research group.

Other porphyrinoid photosensitizers used in the in vitro photodynamic therapy of OSCC cells should also be noted. Thomas et al. investigated the photosensitizing activity of a novel water-soluble porphyrin that possessed 4-sulfonatophenyl rings using SCC-131 and SCC-172 cells.[44] The novel porphyrin showed photocytotoxicity against both cell lines with IC_{50} values of 13 and 11 μM for SCC-131 and SCC-172, respectively. The two other OSCC cell lines—YD10B derived from the tongue and YD38 from the lower gingiva—were used to examine the photocytotoxicity of pheophorbide b.[45] The use of 0.3 μM of this photosensitizer led to the reduction of YD10B cell viability by 70% and of YD38 cell viability by 60%. Other experiments using YD10B cells revealed the photosensitizing activity of the hexenyl ester of 5-aminolevulinic acid, which decreased the cell viability by 85% at 5.0 μM.[46] Non-porphyrinoid photosensitizers were also tested on OSCC cells. Lim et al. examined fifteen different boron bipyrromethene derivatives using HSC-2 cells that originated from the oral floor.[47] Three of them exhibited high photocytotoxicity, with IC_{50} values in the range of 0.1 to 0.6 μM. Lucky et al. prepared titanium oxide coated nanoparticles and examined their in vitro photocytotoxicity on CAL-27 cells.[48] It was found that pegylated TiO_2 nanoparticles decreased cell viability by about 80% at 1.0 mM and about 40% at 10.0 μM. It is worth noting that Pzs **9**, **11**, and **12** at 10.0 μM showed higher photosensitizing effects at the same concentration on CAL-27 cells. The results reported in this study together with literature data led to the conclusion that Pz **12** possesses one of the highest activities in vitro on OSCC cells described so far. It is also worth noting that Pz **9** (G_1 peripheral dendron generation) revealed significantly lower IC_{50} values than that for Pz **11** (G_0 peripheral dendron generation) (Table 2). These results can be analyzed together with the above described singlet-oxygen-generation efficacy with values decreasing in the following order: Pz **12** > Pz **9** > Pz **11** (Table 1).

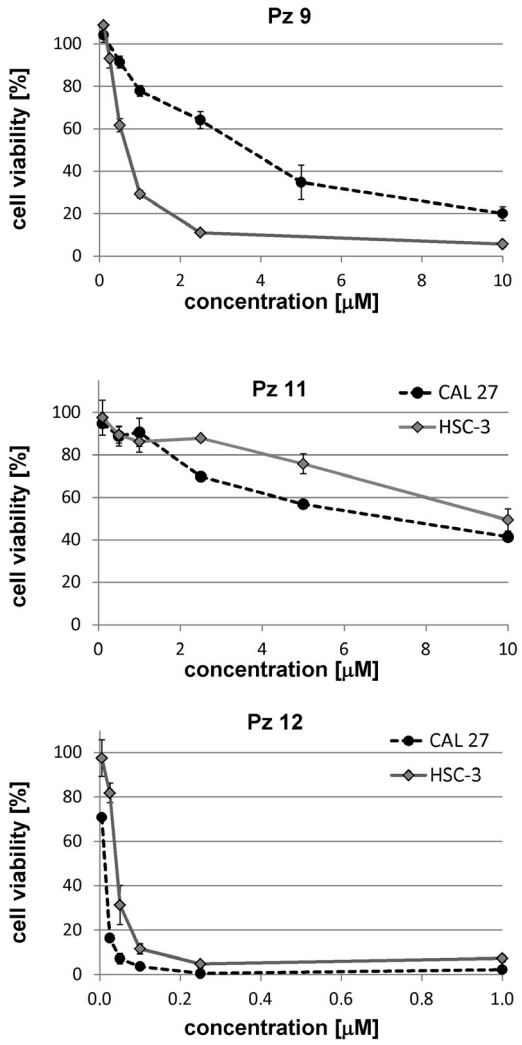

Figure 4. Phototoxic effect of Pzs **9**, **11**, and **12** on CAL 27 and HSC-3 cells. Data represent the mean ± standard deviation for experiments performed in triplicate.

Table 2. IC_{50} values [μM] for the cytotoxicity of the studied photosensitizers.

Pzs	CAL 27	HSC-3
9	3.13	0.64
11	6.66	10.6
12	0.01	0.042

The higher photosensitizing activity of tribenzoporphyrazine **12** relative to Pz **9** and **11** would appear to be connected with its significantly higher singlet-oxygen-generation yield and/or the presence of hydroxyl groups in its periphery, which significantly facilitates its solubility and distribution, rather than with its singlet-oxygen-generation efficacy.

Conclusion

In summary, the synthesis and characterization of sulfanyl porphyrazines and tribenzoporphyrazines substituted in their periphery with different dendrimeric substituents up to their first generation were performed. Under the Linstead macrocyclization reaction conditions, a symmetrical sulfanyl porphyrazine with 3,5-bis(3,5-dimethoxybenzyloxy)benzyl substituents as well as symmetrical porphyrazine and tribenzoporphyrazine with (4-{3,5-bis[3,5-bis(methoxycarbonyl)phenoxymethyl]phenoxy}butylsulfanyl) substituents were obtained. Moreover, novel sulfanyl tribenzoporphyrazine with 4-[3,5-di(butoxycarbonyl)phenoxy]butyl substituents was reduced to tribenzoporphyrazine with 4-[3,5-di(hydroxymethyl)phenoxy]butyl substituents. Further alkylation reaction of this compound with the use of the divergent synthetic approach led to pseudo-G1 sulfanyl dendrimeric tribenzoporphyrazine with 4-(3,5-bis{[4-(3,5-dimethoxycarbonylphenoxy)butoxy]methyl}phenoxy)butyl substituents.

The macrocycles were subjected to photochemical studies in terms of singlet oxygen generation and revealed low or moderate singlet-oxygen-generation efficacy. The sulfanyl tribenzoporphyrazine analogue with terminal hydroxyl groups at the periphery showed the highest ability to generate singlet oxygen ($\Phi_\Delta = 0.20$).

The photodynamic activity of tribenzoporphyrazines was investigated in vitro using two oral squamous cell carcinoma cell lines derived from the tongue (CAL 27, HSC-3). Dark toxicity of tribenzoporphyrazines was not observed in the limited concentration range of 0.1 to 10.0 μM. Therefore, the light-induced toxicity was examined at the same concentrations as the dark toxicity (0.1, 1.0, 10.0 μM). It was found that all compounds at 10.0 μM reduced the viability of both cell lines by 50–95%. Tribenzoporphyrazine with 4-[3,5-di(hydroxymethyl)phenoxy]butyl substituents revealed the highest reduction of the viabilities of CAL 27 and HSC-3 cells above 95% at 1.0 μM. Moreover, the aforementioned tribenzoporphyrazine with 4-(3,5-dibutoxycarbonylphenoxy)butyl substituents decreased the viability of both cell lines at the lowest concentration used (0.1 μM). Further experiments were performed for each compound to evaluate the correlation between cancer-cell viability and the concentration of the photosensitizers. The lowest nanomolar IC_{50} values were obtained with tribenzoporphyrazine with 4-[3,5-di(hydroxymethyl)phenoxy]butyl substituents (10 nM and 42 nM for CAL 27 and HSC-3 cells, respectively). It is worth noting that sulfanyl tribenzoporphyrazine with 4-{3,5-bis[3,5-bis(butoxycarbonyl)phenoxymethyl]phenoxy}butyl substituents (G_1 peripheral dendron generation) revealed significantly lower IC_{50} values than sulfanyl tribenzoporphyrazine with 4-(3,5-dibutoxycarbonylphenoxy)butyl substituents (G_0 peripheral dendron generation). These results can be compared to the singlet-oxygen-generation efficiency. According to the singlet-oxygen-generation efficiency, the sulfanyl tribenzoporhyrazines could be ordered in terms of the applied substituent: 4-[3,5-di(hydroxymethyl)phenoxy]butyl > 4-{3,5-bis[3,5-bis(butoxycarbonyl)phenoxymethyl]phenoxy}butyl > 4-[3,5-di(butoxycarbonyl)phenoxy]butyl. The excellent photocytotoxicity of sulfanyl

tribenzoporphyrazine with 4-[3,5-di(hydroxymethyl)phenoxy]-butyl substituents seems to be related more to the presence of hydroxyl groups in its periphery, which significantly facilitates its solubility and distribution, than with its singlet-oxygen-generation efficacy.

Experimental Section

General procedures

All reactions were conducted in oven-dried glassware under an argon atmosphere using a Radleys Heat-On heating system unless otherwise stated. All solvents were rotary evaporated at or below 50 °C under reduced pressure. All solvents and reagents were obtained from commercial suppliers and used without further purification unless otherwise stated. Dry flash column chromatography was carried out on Merck silica gel 60 (particle size 40–63 μm) and reversed-phase chromatography on Fluka C_{18} silica gel 90 (particle size 40–63). Thin-layer chromatography (TLC) was performed on silica gel Merck Kieselgel 60 F_{254} plates and visualized by means of UV spectroscopy (λ_{max} = 254 or 365 nm). UV/Vis spectra were recorded with Hitachi UV/VIS U-1900 or Shimadzu PC160 spectrophotometers. The NMR spectra were acquired at 298 K with an Agilent DD2 800 NMR spectrometer operating at resonance frequencies of 799.903 and 201.146 MHz for ^{1}H and ^{13}C, respectively. Chemical shifts (δ) are quoted in parts per million (ppm) and are referred to a residual solvent peak. Coupling constants (J) are quoted in Hertz (Hz). The abbreviations s, p, t, h, and m refer to singlet, pentet, triplet, hidden, and multiplet, respectively. The ^{1}H and ^{13}C NMR spectroscopic resonances were assigned using a combination of homo- and heteronuclear two-dimensional techniques such as ^{1}H–^{1}H COSY, ^{1}H–^{13}C HSQC, and ^{1}H–^{13}C HMBC. Mass spectra (ES, MALDI TOF, HRMS) and combustion analyses were carried out by the Advanced Chemical Equipment and Instrumentation Facility at the Faculty of Chemistry and the Wielkopolska Center for Advanced Technologies at Adam Mickiewicz University in Poznan, and at the European Center of Bioinformatics and Genomics in Poznan. Melting point was obtained using a "Stuart" Bibby apparatus and is uncorrected. Analytical HPLC was carried out using an Agilent 1200 instrument equipped with a UV-DAD detector. The chromatographic separation was achieved on an octadecylsilane-coated column (150 mm × 4.6 mm, 5 μm; Eclipse XDB-C18, Agilent) or on hexaphenyl-coated columns (150 mm × 4.6 mm, 5 μm or 250 mm × 4.6 mm, 5 μm; Gemini C6-Phenyl, Phenomenex) under isocratic and linear gradient conditions.

Synthetic procedures

3,5-Bis(3,5-dimethoxybenzyloxy)benzyl bromide (**2**) was purchased from TCI Chemicals (Tokio, Japan). 3,5-Bis[3,5-bis(methoxycarbonyl)-phenoxymethyl]phenol (**5**) was synthesized according to the procedure described by Höger.[28] 2,3-Bis[4-(3,5-dimethoxycarbonylphenoxy)butylsulfanyl] maleonitrile (**10**) was synthesized according to the previously published procedure.[25]

Synthetic procedure leading to symmetrical porphyrazine 4

2,3-Bis[3,5-bis(3,5-dimethoxybenzyloxy)benzylsulfanyl]maleonitrile (3): Dimercaptomaleonitrile disodium salt (100 mg, 0.54 mmol), 3,5-bis(3,5-dimethoxybenzyloxy)benzyl bromide (**2**) (673 mg, 1.34 mmol), and K_2CO_3 (296 mg, 2.15 mmol) in anhydrous DMF (10 mL) were stirred at room temperature for 48 h. Next, the reaction mixture was filtered through Celite, which was then washed with CH_2Cl_2. The filtrate was evaporated and the solid residue was chromatographed (CH_2Cl_2/methanol 100:1 to 50:1) to give **3** as a yellow oil (471 mg, 89%); R_f = 0.55 (CH_2Cl_2/methanol 100:1); ^{1}H NMR (800 MHz, [D$_6$]DMSO): δ = 6.65 (d, ^4J = 2 Hz, 4H; C2′, C6′ ArH), 6.60 (t, ^4J = 2 Hz, 2H; C4′, ArH), 6.57 (d, ^4J = 2 Hz, 8H; C2″, C6″, $ArOCH_3$), 6.43 (t, ^4J = 2 Hz, 4H; C4″, $ArOCH_3$), 4.98 (s, 8H; OCH_2), 4.39 (s, 4H; SCH_2), 3.72 ppm (s, 24H; OCH_3); ^{13}C NMR (201 MHz, [D$_6$]DMSO): δ = 160.5 (C3″, C5″, $ArOCH_3$), 159.5 (C3′, C5′, ArC), 139.1 (C1″, $ArOCH_3$), 137.3 (C1′, ArC), 120.9 (CS), 112.5 (CN), 108.1 (C2′, C6′, ArC), 105.4 (C2″, C6″, $ArOCH_3$) 101.4 (C4′, ArC), 99.5 (C4″, $ArOCH_3$), 69.2 (OCH_2) 55.1 (CH_3), 38.2 ppm (SCH_2); UV/Vis (CH_2Cl_2): λ_{max} (log ε) = 280 (4.33), 349 nm (4.23); MS (MALDI): *m/z*: 987 [*M*+H]$^+$, 1009 [*M*+Na]$^+$, 1025 [*M*+K]$^+$; HRMS (ESI): *m/z* calcd. ($C_{54}H_{55}N_2O_{12}S_2$): 987.3196 [*M*+H]$^+$; found: 987.3195 [*M*+H]$^+$; elemental analysis calcd. for $C_{54}H_{55}N_2O_{12}S_2 \times 0.5\,H_2O$: C 65.11 H, 5.57, N 2.81, S 6.44; found: C 64.74, H 6.04, N 2.67, S 5.99.

2,3,7,8,12,13,17,18-Octakis[3,5-bis(3,5-dimethoxybenzyloxy)benzylthio]porphyrazinato magnesium(II) (4): Magnesium turnings (5.0 mg, 0.2 mmol) and a small crystal of iodine were heated to reflux in *n*-butanol (2.0 mL) for 4 h. After cooling to room temperature, the reaction mixture was transferred using a syringe to a flask that contained **3** (197 mg, 0.20 mmol). Then the reaction mixture was heated under reflux conditions for another 20 h. Next, the reaction mixture was cooled to room temperature, filtered through Celite, then washed with toluene and CH_2Cl_2. Filtrates were evaporated to dryness, and a dark blue residue was chromatographed using silica gel (CH_2Cl_2/methanol 100:1 to 20:1) then reversed-phase column chromatography (methanol, then CH_2Cl_2) to give **4** as a blue film (71 mg, 36%). M.p. > 50 °C (mesophase behavior); R_f = 0.46 (CH_2Cl_2/methanol 50:1); ^{1}H NMR (800 MHz, [D$_5$]pyridine): δ = 7.28 (d, ^4J = 2 Hz, 16H; C2′, C6′, ArH), 6.83 (t, ^4J = 2 Hz, 8H; C4′, ArH), 6.71 (d, ^4J = 2 Hz, 32H; C2″, C6″, $ArOCH_3$), 6.59 (t, ^4J = 2 Hz, 16H; C4″, $ArOCH_3$), 5.72 (s, 32H; OCH_2), 4.90 ppm (s, 16H; SCH_2), 3.68 s, 96H; OCH_3); ^{13}C NMR (201 MHz, [D$_5$]pyridine): δ = 161.9 (C3″, C5″, $ArOCH_3$), 161.2 (C3′, C5′, ArC), 158.5 (C1, C4, pyrrole C), 142.1 (C1′, ArC), 141.7 (C2, C3, pyrrole C), 140.3 (C1″, $ArOCH_3$), 109.5 (C2′, C6′, ArC), 106.3 (C2″, C6″, $ArOCH_3$), 102.5 (C4′, ArC) 100.8 (C4″, $ArOCH_3$), 70.7 (OCH_2), 55.8 (OCH_3), 41.3 ppm (SCH_2); UV/Vis (CH_2Cl_2): λ_{max} (log ε) = 280 (4.89), 370 (4.78), 676 nm (4.80); MS (MALDI): *m/z*: 3995 [*M*+Na]$^+$; HRMS (ESI): *m/z* calcd. ($C_{216}H_{217}MgN_8O_{48}S_8$): 3970.2401 [*M*+H]$^+$; found: 3970.2151 [*M*+H]$^+$. For HPLC purity, see the Supporting Information.

Synthetic procedure leading to symmetrical porphyrazine 8 and tribenzoporphyrazine 9

1-(4-Bromobutoxy)-3,5-bis[3,5-bis(methoxycarbonyl)phenoxymethyl]benzene (6): 3,5-Bis[3,5-bis(methoxycarbonyl)phenoxymethyl]-phenol (0.464 g, 0.86 mmol), 1,4-dibromobutane (0.31 mL, 2.59 mmol), and potassium carbonate (3.6 g, 25.9 mmol) in anhydrous DMF (6 mL) were stirred at 50 °C for 22 h. Next, the reaction mixture was filtered through Celite, then washed with CH_2Cl_2. The filtrate was evaporated and the solid residue was chromatographed (CH_2Cl_2) to give **6** as a white powder (434 mg, 75%). M.p. 129 °C; R_f = 0.36 (CH_2Cl_2/methanol 50:1); ^{1}H NMR (800 MHz, [D$_6$]DMSO): δ = 8.06 (t, ^4J = 1 Hz, 2H; C4′, ArH), 7.73 (d, ^4J = 1 Hz, 4H; C2′, C6′, ArH), 7.12 (s, 1H; C4, ArH), 7.02 (s, 2H; C2, C6, ArH), 5.23 (s, 4H; $ArCH_2O$), 4.04 (t, ^3J = 6 Hz, 2H; CH_2CH_2O), 3.88 (s, 12H; OCH_3), 3.60 (t, ^3J = 7 Hz, 2H; $BrCH_2$), 1.97 (m, 2H; $BrCH_2CH_2$), 1.84 ppm (m, 2H; CH_2CH_2O); ^{13}C NMR (201 MHz, [D$_6$]DMSO): δ = 165.1 (C=O), 158.7 (C1, ArC), 158.4 (C1′, ArC), 138.2 (C3, C5, ArC),

131.5 (C3′, C5′, ArC), 121.9 (C4′, ArC), 119.6 (C2′, C6′, ArC), 118.3 (C4, ArC), 113.0 (C2, C6, ArC), 69.4 ($ArCH_2O$), 66.7 (CH_2CH_2O), 52.5 (OCH_3), 34.8 ($BrCH_2$), 29.0 ($BrCH_2CH_2$), 27.3 ppm (CH_2CH_2O); UV/Vis (CH_2Cl_2): λ_{max} ($\log\varepsilon$) = 286 (3.67), 307 nm (3.83); MS (ES+): *m/z*: 671, 673 $[M+H]^+$, 695, 697 $[M+Na]^+$, 711, 713 $[M+K]^+$; MS (ES−): *m/z*: 707, 709 $[M+Cl]^-$; elemental analysis calcd. for $C_{32}H_{33}BrO_{11}\cdot H_2O$: C 55.58, H 5.10; found: C 55.53, H 5.14.

2,3-Bis(4-{3,5-bis[3,5-bis(methoxycarbonyl)phenoxymethyl]phenoxy}butylsulfanyl)maleonitrile (7): Dimercaptomaleonitrile disodium salt (52 mg, 0.28 mmol), **6** (434 mg, 0.64 mmol), and potassium carbonate (300 mg, 2.17 mmol) were stirred in anhydrous DMF (5 mL) at 50 °C for 21 h. The solvent was evaporated, and the residual oil was chromatographed (CH_2Cl_2/methanol 50:1 to 35:1) to give **7** as a yellow oil (317 mg, 85% yield). R_f = 0.11 (CH_2Cl_2/methanol 50:1); ^{1}H NMR (800 MHz, [D$_6$]DMSO): δ = 7.99 (d, ^4J = 1 Hz, 4H; C4″, ArH), 7.67 (t, ^4J = 1 Hz, 8H; C2″, C6″, ArH), 7.09 (s, 2H; C4′, ArH), 6.96 (s, 4H; C2′, C6′, ArH), 5.15 (s, 8H; $ArCH_2O$), 3.99 (t, ^3J = 6 Hz, 4H; CH_2CH_2O), 3.85 (s, 24H; OCH_3), 3.23 (t, ^3J = 7 Hz, 4H; SCH_2), 1.81 ppm (br s, 8H; $CH_2CH_2CH_2O$); ^{13}C NMR (201 MHz, [D$_6$]DMSO): δ = 165.0 (C=O), 158.7 (C1′, ArC), 158.3 (C1″, ArC), 138.1 (C3′, C5′, ArC), 131.3 (C3″, C5″, ArC), 121.9 (CS), 121.4 (C4″, ArC), 119.5, (C2″, C6″, ArC), 118.2 (C4′, ArC), 112.9 (C2′, C6′, ArC), 112.4 (NC), 69.4 (C3′CH_2O), 66.8 ($SCH_2CH_2CH_2CH_2$), 52.4 (OCH_3), 34.2 (SCH_2), 27.2 (SCH_2CH_2), 26.1 ppm ($SCH_2CH_2CH_2$); UV/Vis (CH_2Cl_2): λ_{max} ($\log\varepsilon$) = 285 (4.14), 315 (4.30), 343 ppm (4.22); MS (MALDI): *m/z*: 1327 $[M+H]^+$, 1349 $[M+Na]^+$, 1365 $[M+K]^+$; elemental analysis calcd. for $C_{68}H_{66}N_2O_{22}S_2$: C 61.53, H 5.01, N 2.11, S 4.83; found: C 61.09, H 5.02, N 2.07, S 4.74.

2,3,7,8,12,13,17,18-Octakis(4-{3,5-bis[3,5-bis(butoxycarbonyl)-phenoxymethyl]phenoxy}butylthio)porphyrazinato magnesium(II) (8): Magnesium turnings (6 mg, 0.25 mmol) and a small crystal of iodine were heated to reflux in *n*-butanol (2.5 mL) for 2 h. After cooling to room temperature, the reaction mixture was transferred using a syringe to a flask that contained maleonitrile **7** (334 mg, 0.25 mmol) and was heated under reflux conditions for 22 h. Next, the reaction mixture was cooled to room temperature, filtered through Celite, then washed with toluene. Filtrates were evaporated in a rotary evaporator, which resulted in a dark blue residue, which was chromatographed using silica gel (CH_2Cl_2/methanol, 50:1 v/v) and reversed-phase column chromatography (methanol, than CH_2Cl_2), then silica gel once again (*n*-hexane/ethyl acetate, 7:3 v/v) to give **8** as a dark blue film (95 mg; 23% yield). M.p. > 235 °C decomp; R_f = 0.28 (*n*-hexane/ethyl acetate, 7:3); ^{1}H NMR (800 MHz, [D$_5$]pyridine): δ = 8.57 (s, 16H; C4″, ArH), 8.07 (s, 32H; C2″, C6″, ArH), 7.39 (s, 8H; C4′, ArH), 7.20 (sh, 16H; C2′, C6′, ArH), 5.22 (s, 32H; C3′CH_2O), 4.59 (s, 16H; SCH_2), 4.37 (t, ^3J = 7 Hz, 64H; $COOCH_2$), 4.19 (s, 16H; $ArOCH_2CH_2$), 2.37 (br s, 32H; $SCH_2CH_2CH_2$), 1.66 (m, 64H; $COOCH_2CH_2$), 1.37 (m, 64H; CH_3CH_2), 0.88 ppm (m, 96H; CH_3); ^{13}C NMR (201 MHz, [D$_5$]pyridine): δ = 166.0 (C=O), 160.5 (C1′, ArC), 159.7 (C1″, ArC), 139.3 (C3′, C5′, ArC), 133.2 (C3″, C5″, ArC), 123.7 (C4″, ArC), 120.7 (C2″, C6″, ArC), 119.6 (C4′, ArC), 114.2 (C2′, C6′, ArC), 70.8 ($ArCH_2O$), 68.5 ($ArOCH_2CH_2$), 65.9 ($COOCH_2$), 35.9 (SCH_2), 31.4 ($COOCH_2CH_2$), 29.6 ($SCH_2CH_2CH_2$), 28.1 (SCH_2CH_2), 19.9 (CH_3CH_2), 14.3 ppm (CH_3); UV/Vis (CH_2Cl_2): λ_{max} ($\log\varepsilon$) = 673 (4.50), 374 (4.62), 314 (4.67), 286 nm (4.52); MS (MALDI): *m/z*: 6677 $[M+H]^+$; HRMS (MALDI): *m/z*: calcd. ($C_{368}H_{457}MgN_8O_{88}S_8$): 6675.915; found: 6675.762. For HPLC purity, see the Supporting Information.

22,23-Bis(4-{3,5-bis[3,5-bis(butoxycarbonyl)phenoxymethyl]phenoxy}butylthio)tribenzo[*b*,*g*,*l*]porphyrazinato magnesium(II) (9): Magnesium turnings (13 mg, 0.512 mmol) were heated to reflux in *n*-butanol (15 mL) with a small crystal of iodine for 6 h in a round-bottomed flask. After cooling, the contents of the flask were transferred with a syringe to another round-bottomed flask that contained maleonitrile derivative **7** (136 mg, 0.102 mmol) and 1,2-dicyanobenzene (131 mg, 1.024 mmol), then it was heated to reflux for another 20 h. The resulting blue product was filtered through Celite with toluene, and the solvents were evaporated under reduced pressure. Compound **9** was purified by means of column chromatography using silica gel and *n*-hexane/ethyl acetate (7:2) to give 82 mg of a blue film (39% yield). M.p. 87–89 °C; R_f = 0.15 (CH_2Cl_2/MeOH 35:1); ^{1}H NMR (800 MHz, [D$_5$]pyridine): δ = 9.62–9.17 (m, 8H; tribenzo-H), 8.61–8.47 (m, 6H; isophthalo-H), 8.25–8.13 (m, 4H; tribenzo-H), 8.12–7.79 (m, 12H; isophthalo-H), 5.31–5.03 (m, 8H; OCH_2Ph), 4.78 (br s, 4H; SCH_2), 4.36–4.23 (m, 20H; OCH_2CH_2), 1.65–1.52 (m, 20H; $SCH_2CH_2CH_2$), 1.39–1.25 (m, 20H; $SCH_2CH_2CH_2$, CH_2CH_3), 0.86–0.75 ppm (m, 24H; CH_3); ^{13}C NMR (201 MHz, [D$_5$]pyridine): δ = 167.9, 161.8, 161.6, 161.5, 152.6, 142.9, 141.4, 140.7, 138.2, 136.5, 136.4, 135.3, 135.2, 135.1, 133.9, 131.7, 126.2, 125.6, 122.7, 122.6, 122.4, 72.9, 72.6, 72.4, 70.6, 67.8, 41.5, 33.8, 33.3, 32.4, 31.6, 26.5, 25.6, 21.8, 16.2; UV/Vis (CH_2Cl_2): λ_{max} ($\log\varepsilon$) = 694 (3.73), 651 (3.63), 359 (3.64), 316 nm (3.66); MS (MALDI TOF): *m/z*: 2071.871 $[M+H]^+$; HRMS (ESI): *m/z*: calcd. ($C_{116}H_{126}MgN_8O_{22}S_2$): 2070.82786 $[M]^+$; found: 2070.84590 $[M]^+$. For HPLC purity, see the Supporting Information.

Synthetic procedure leading to tribenzoporphyrazines 11–13

22,23-Bis[4-(3,5-dibutoxycarbonylphenoxy)butylthio]tribenzo[*b*,*g*,*l*]porphyrazinato magnesium(II) (11): Magnesium turnings (100 mg, 4.098 mmol) were heated to reflux in *n*-butanol (40 mL) with a small crystal of iodine for 6 h in a round-bottomed flask. After cooling, the contents of the flask were transferred with a syringe to another round-bottomed flask that contained maleonitrile derivative **6** (500 mg, 0.745 mmol) and 1,2-dicyanobenzene (955 mg, 7.450 mmol), the heated to reflux for another 20 h. The resulting blue product was filtered through Celite with toluene, and the solvents were evaporated under reduced pressure. Compound **11** was purified by means of column chromatography using silica gel and *n*-hexane/ethyl acetate (7:2) to give 307 mg of a blue film (33% yield). M.p. 138–140 °C; R_f = 0.07 (CH_2Cl_2/MeOH 50:1); ^{1}H NMR (800 MHz, [D$_6$]DMSO): δ = 9.29, 9.28 (2d, J = 5 Hz, 2H; tribenzo-H), 9.24 (d, J = 7 Hz, 2H; tribenzo-H), 9.14 (d, ^3J = 7 Hz, 2H; tribenzo-H), 8.20, 8.19 (2d, J = 5 Hz, 2H; tribenzo-H), 8.12, 8.10 (2t, J = 6 Hz, 4H; tribenzo-H), 7.23 (s, 2H; isophthalate-H), 6.69 (s, 4H; isophthalate-H), 4.33 (t, ^3J = 7 Hz, 4H; $PhOCH_2$), 3.85 (t, ^3J = 7 Hz, 8H; $C(O)OCH_2$), 3.75 (t, ^3J = 6 Hz, 4H; SCH_2), 1.97 (m, 8H; $SCH_2CH_2CH_2$), 1.35 (m, 8H; $CH_2CH_2CH_3$), 1.16 (m, 8H; CH_2CH_3), 0.74 ppm (t, ^3J = 7 Hz, 12H; CH_3); ^{13}C NMR (201 MHz, [D$_6$]DMSO): δ = 167.8, 166.9 (C=O), 160.9 (isophthalate), 159.9, 159.4, 155.9, 154.9, 142.1, 142.0, 141.3, 139.9, 134.8, 133.6 (isophthalate), 133.4, 133.1, 132.5, 126.0, 125.9, 123.8 (isophthalate), 121.0 (isophthalate), 69.9 (SCH_2), 67.5 ($C(O)OCH_2$), 37.1 ($PhOCH_2$), 33.0 ($CH_2CH_2CH_3$), 30.4, 29.5 ($SCH_2CH_2CH_2$), 21.6 (CH_2CH_3), 16.5 ppm (CH_3); UV/Vis ($CHCl_3$): λ_{max} ($\log\varepsilon$) = 721 (3.62), 626 (3.54), 357 nm (3.76); MS (MALDI-TOF): *m/z*: 1247.403 $[M+H]^+$; HRMS (ESI): *m/z*: calcd. ($C_{68}H_{71}MgN_8O_{10}S_8$): 1247.45795 $[M+H]^+$; found: 1247.45862 $[M+H]^+$. For HPLC purity, see the Supporting Information.

22,23-Bis{4-[3,5-di(hydroxymethyl)phenoxy]butylthio}tribenzo[*b*,*g*,*l*]porphyrazinato magnesium(II) (12): $LiAlH_4$ (44 mg, 1.152 mmol) was suspended in THF (10 mL) and stirred for 0.5 h at 0 °C. After that, a solution of **11** (300 mg, 0.240 mmol) in THF (6 mL) was added dropwise over 40 min. Next, the ice bath was removed, and the reaction mixture was left to warm to room tem-

perature and was stirred for 2 h. The reaction was quenched with saturated NH_4Cl solution (10 mL) and left for another 15 min. The reaction mixture was filtered through Celite, then washed with CH_2Cl_2. The filtrates were evaporated to dryness. Column chromatography (CH_2Cl_2, then CH_2Cl_2/MeOH 20:1) led to **12** in the form of a deep blue film (150 mg, 65% yield). M.p. 151–153 °C; R_f = 0.12 (CH_2Cl_2/MeOH 10:1); ^{1}H NMR (800 MHz, [D_5]pyridine): δ = 9.57–8.84 (m, 4H; tribenzo-H, isophthalo-H), 8.64–7.57 (m, 12H; tribenzo-H, isophthalo-H), 7.51–7.21 (m, 2H; tribenzo-H, isophthal-H), 4.34 (m, 4H; O*CH*$_2$CH$_2$), 4.07–3.81 (m, 4H; SCH$_2$), 1.62 (m, 4H; S-CH$_2$-CH$_2$-*CH*$_2$), 1.33 (m, 4H; S-CH$_2$-*CH*$_2$), 0.83 ppm (m, 8H; *CH*$_2$OH); ^{13}C NMR (201 MHz, [D_5]pyridine): δ = 161.9, 156.0, 155.9, 154.8, 146.4, 132.0, 130.3, 129.9, 128.9, 126.0, 125.7, 120.0, 119.0, 116.1, 100.3, 63.1, 61.5, 27.1, 15.5, 10.0 ppm; UV/Vis (CH_2Cl_2): λ_{max} (log ε) = 711 (3.81), 652 (3.26), 597 (3.29), 382 nm (3.55); MS (MALDI TOF): *m/z* 967.181 [*M*]$^+$. For HPLC purity, see the Supporting Information.

22,23-Bis[4-(3,5-bis{[4-(3,5-dimethoxycarbonylphenoxy)butoxy]-methyl}phenoxy)butylthio]tribenzo[*b*,*g*,*l*]porphyrazinato magnesium(II) (13): Porphyrazine derivative **12** (74 mg, 0.076 mmol), dimethyl 5-(4-bromobutoxy)benzene-1,3-dicarboxylate (132 mg, 0.382 mmol), and cesium carbonate (248 mg, 0.761 mmol) were stirred in DMF (15 mL) at 60 °C for 19 h. After cooling, the reaction mixture was filtered through Celite, then washed with toluene. The filtrates were evaporated under reduced pressure to yield the dry residue. Column chromatography was performed (CH_2Cl_2/MeOH 20:1) to give **10** as a dark blue film (31 mg, 20% yield). M.p. 133–135 °C; R_f = 0.12 (CH_2Cl_2/MeOH 20:1); ^{1}H NMR (800 MHz, [D_5]pyridine): δ = 9.57 (m, 6H; tribenzo-H), 8.55–8.39 (m, 6H; tribenzo-H), 8.13 (m, 6H; isophthal-H), 7.95–7.77 (m, 12H; isophthal-H), 4.49–4.37 (m, 8H; Ph–*CH*$_2$–O), 4.04–3.91 (m, 12H; Ph–O–*CH*$_2$), 3.83 (m, 24H; *CH*$_3$), 2.30 (d, *J* = 13 Hz, 4H; S–*CH*$_2$), 1.94–1.84, 1.30–1.20 ppm (m, 24H; CH$_2$–*CH*$_2$–*CH*$_2$–CH$_2$); ^{13}C NMR (201 MHz, [D_5]pyridine): δ = 166.4, 166.0, 159.9, 150.6, 136.2, 134.5, 132.7, 124.2, 123.3, 120.4, 68.6, 67.6, 65.8, 62.2, 52.8, 30.4, 26.5, 26.1 ppm; UV/Vis ($CHCl_3$): λ_{max} (log ε) = 694 (3.37), 651 (3.63), 359 (3.64), 316 nm (3.66); MS (MALDI TOF): *m/z*: 2024.679 [*M*+H]$^+$. For HPLC purity, see the Supporting Information.

Singlet-oxygen measurements and spectroscopic studies

The evaluation of singlet oxygen generation for the examined compounds was performed in DMF according to the methodology previously described.[35–37] 1,3-Diphenylisobenzofuran (DPBF) was used as a singlet-oxygen chemical quencher (Sigma–Aldrich). Unsubstituted zincphthalocyanine (ZnPc) with known singlet-oxygen quantum yields (0.56 and 0.67 in DMF and DMSO, respectively) was used as a reference.

Biological studies

Cell culture

Oral squamous cell carcinoma cell lines derived from the tongue (CAL 27, HSC-3) were purchased from ATCC (Teddington, UK) for CAL 27 or provided by Dr. R. Kramer (University of California, San Francisco, UCSF, USA) for HSC-3.[49] The cells were cultured in Dulbecco's modified Eagle medium (DMEM), supplemented with 10% (v/v) heat-inactivated fetal bovine serum (FBS), penicillin (100 U mL^{-1}), streptomycin (100 μg mL^{-1}), and L-glutamine (4 mM) (DMEM/10). The cells were incubated in tissue culture flasks at 37 °C in a humidified atmosphere that contained 5% CO_2, then were passaged 1:6 (HSC-3) or 1:4 (CAL 27) twice a week using a Trypsin-EDTA solution. All media—that is, penicillin-streptomycin solution, L-glutamine, FBS, Trypsin-EDTA, phosphate buffered saline (PBS), Dulbecco's phosphate buffered saline (DPBS)—were obtained from the UCSF Cell Culture Facility, San Francisco, USA. Photosensitizers were dissolved in dimethyl sulfoxide (Sigma–Aldrich) and subsequently diluted in DMEM (without FBS and phenol red) to obtain the desired concentration of photosensitizer used in the experiments. The DMSO concentration in the final solution did not exceed 0.5%.

Dark toxicity

One day before the experiment, the cells were seeded in 48-well plates at a density 1.8×10^5 in 1 mL of medium in each well (with FBS and phenol red) and used at approximately 80% confluence. Subsequently, the cells were washed with PBS (1 mL), and the medium (1 mL; without FBS and phenol red) that contained the photosensitizer at a given concentration was added to each well except for the controls. The FBS-free media were used to avoid binding of photosensitizers to serum proteins. After a 24 h incubation at 37 °C, the cells were washed with PBS, then complete medium (1 mL) was added to each well, and the cells were incubated for 24 h at 37 °C. The cell viability was quantified by the Alamar Blue assay. The cells incubated either with medium alone or in medium/0.5% DMSO served as controls.

Light-dependent toxicity

One day before the experiment, the CAL 27 and HSC-3 cells were seeded in 48-well plates at a density 1.8×10^5 cells per well, respectively, in complete medium (1 mL), and used at approximately 80% confluence. The cells were washed with PBS (1 mL). Next, the medium (1 mL; without FBS and phenol red) that contained the photosensitizer was added to each well except for the controls. After washing, controls were treated with the same medium without photosensitizers. The cells were incubated for 24 h at 37 °C, washed with PBS, and irradiated for 20 min with light at a wavelength of 690 nm from a High Power LED Multi Chip Emitter (Roithner Lasertechnik, 9.8 V). The light intensity at the surface of the plate was set to 3.0 mW cm^{-2} as measured by a Thorlabs TM100A Optical Power Meter, and the total light dose was 3.6 J cm^{-2}. One plate from each experiment was not exposed to light and served as a control. Directly after light exposure, the medium without FBS and phenol red was replaced with 1 mL of complete medium, and the cells were incubated for 24 h at 37 °C. Cell viability was quantified by the Alamar Blue assay.

Cell viability

Cell morphology was evaluated using a Nikon TMS inverted-phase contrast microscope at 100× magnification. The number of viable cells used for the experiments was determined by the Trypan Blue exclusion assay (Gibco-Invitrogen Corporation). The cell viability was quantified by a modified Alamar Blue assay.[50,51] Briefly, 10% (v/v) Alamar Blue dye (1 mL) in the appropriate complete medium was added to each well. After incubation at 37 °C for 2–3 hours; the supernatant (200 μL) was assayed by measuring the absorbance at 570 and 600 nm. The cell viability (as a percentage of control cells) was calculated according to the formula [Eq. (1)]:

$$\text{Cell viability} = [(\text{A570} - \text{A600})\ \text{of test cells}] \times 100/[(\text{A570} - \text{A600})\text{of control cells}] \quad (1)$$

Statistical analysis

Statistical analyses were performed with one-way analysis of variance (ANOVA) followed by Dunnett's multiple comparison test by using GraphPad Prism version 5.00 for Windows (GraphPad Software, San Diego, California, USA). The results were presented as the mean ± standard deviation (SD) from experiments performed in triplicate. A probability value (p) of less than 0.05 was considered significantly different.

Acknowledgements

This study was supported by the National Science Centre under grant no. 2012/05/E/NZ7/01204. L.P. and S.J. acknowledge financial support from the National Centre for Research and Development under grant no. PBS1/A9/13/2012. The authors thank Beata Kwiatkowska, Rita Kuba, Jennifer Cheung, and Ryan Yu for excellent technical assistance. K.K. and N.D. acknowledge funds from the University of the Pacific, Arthur A. Dugoni School of Dentistry.

Keywords: dendrimers · NMR spectroscopy · photochemistry · porphyrazine · singlet oxygen

[1] M. S. Rodríguez-Morgade, P. A. Stuzhin, *J. Porphyrins Phthalocyanines* **2004**, *8*, 1129 – 1165.
[2] J. Piskorz, K. Konopka, N. Düzgüneş, Z. Gdaniec, J. Mielcarek, T. Goslinski, *ChemMedChem* **2014**, *9*, 1775 – 1782.
[3] E. R. Trivedi, C. M. Blumenfeld, T. Wielgos, S. Pokropinski, P. Dande, T. T. Hai, A. G. M. Barrett, B. M. Hoffman, *Tetrahedron Lett.* **2012**, *53*, 5475 – 5478.
[4] L. Chen, Z. Zhanga, Y. Wanga, Y. Guana, K. Denga, K. Lva, J. Suna, Z. Lia, M. Li, *J. Mol. Catal. A* **2013**, *372*, 114 – 120.
[5] T. Goslinski, E. Tykarska, M. Kryjewski, T. Osmałek, S. Sobiak, M. Gdaniec, Z. Dutkiewicz, J. Mielcarek, *Anal. Sci.* **2011**, *27*, 511 – 515.
[6] S. Ristori, G. Ricciardi, D. Pietrangeli, A. Rosa, A. Feis, *J. Phys. Chem. C* **2009**, *113*, 8537 – 8540.
[7] Y. Song, H. Zong, E. R. Trivedi, B. J. Vesper, E. A. Waters, A. G. M. Barrett, J. A. Radosevich, B. M. Hoffman, T. J. Meade, *Bioconjugate Chem.* **2010**, *21*, 2267 – 2275.
[8] E. Gonca, Y. Köseoğlu, B. Aktas, A. Gül, *Polyhedron* **2004**, *23*, 1845 – 1849.
[9] S. Lee, B. J. Vesper, H. Zong, N. D. Hammer, K. M. Elseth, A. G. M. Barrett, B. M. Hoffman, J. A. Radosevich, *Met.-Based Drugs* **2008**, *2008*, 391418.
[10] H. Karadeniz, Y. Gök, H. Kantekin, *Dyes Pigm.* **2007**, *75*, 498 – 504.
[11] R. Hou, B. Li, K. Zhong, H. Li, L.-Y. Jin, B. Yin, *Eur. J. Org. Chem.* **2012**, 1138 – 1146.
[12] N. Kabay, Y. Baygu, H. K. Alpoguz, A. Kaya, Y. Gök, *Dyes Pigm.* **2013**, *96*, 372 – 376.
[13] R. Hou, H. Qiu, T. Chen, B. Yin, *Heterocycles* **2009**, *78*, 1799 – 1805.
[14] R. Öztürk, A. Gül, *Tetrahedron Lett.* **2004**, *45*, 947 – 949.
[15] H. Akkus, A. Gül, *Transition Met. Chem.* **2001**, *26*, 689 – 694.
[16] S. Lijewski, J. Piskorz, M. Kucinska, M. Wierzchowski, K. Czerniak, H. Biller, M. Murias, J. Mielcarek, T. Goslinski, *Inorg. Chem. Commun.* **2013**, *29*, 97 – 100.
[17] F. Figueira, P. M. R. Pereira, S. Silva, J. A. S. Cavaleiro, J. P. C. Tomé, *Curr. Org. Synth.* **2014**, *11*, 110 – 126.
[18] W.-S. Li, T. Aida, *Chem. Rev.* **2009**, *109*, 6047 – 6076.
[19] J. Leclaire, R. Dagiral, A. Pla-Quintana, A.-M. Caminade, J.-P. Majoral, *Eur. J. Inorg. Chem.* **2007**, 2890 – 2896.
[20] M. Labieniec-Watala, C. Watala, *J. Pharm. Sci.* **2015**, *104*, 2 – 14.
[21] B. Klajnert, M. Rozanek, M. Bryszewska, *Curr. Med. Chem.* **2012**, *19*, 4903 – 4912.
[22] U. H. Sk, C. Kojima, *BioMol Concepts* **2015**, *6*, 205 – 217.
[23] F. Setaro, R. Ruiz-González, S. Nonell, U. Hahn, T. Torres, *J. Inorg. Biochem.* **2014**, *136*, 170 – 176.
[24] N. C. S. Vieira, A. Figueiredo, A. A. A. de Queiroz, V. Zucolotto, F. E. G. Guimarães, *Sensors* **2011**, *11*, 9442 – 9449.
[25] S. Lijewski, M. Gierszewski, L. Sobotta, J. Piskorz, P. Kordas, M. Kucinska, D. Baranowski, Z. Gdaniec, M. Murias, J. Karolczak, M. Sikorski, J. Mielcarek, T. Goslinski, *Dyes Pigm.* **2015**, *113*, 702 – 708.
[26] T. Rebis, S. Lijewski, J. Nowicka, L. Popenda, L. Sobotta, S. Jurga, J. Mielcarek, G. Milczarek, T. Goslinski, *Electrochim. Acta* **2015**, *168*, 216 – 224.
[27] R. P. Linstead, M. Whalley, *J. Chem. Soc.* **1952**, 4839 – 4846.
[28] S. Höger, *Synthesis* **1997**, 20 – 22.
[29] T. P. Forsyth, D. B. G. Williams, A. G. Montalban, C. L. Stern, A. G. M. Barrett, B. M. Hoffman, *J. Org. Chem.* **1998**, *63*, 331 – 336.
[30] L. Zhu, M. Lu, D. Qu, Q. Wang, H. Tian, *Org. Biomol. Chem.* **2011**, *9*, 4226 – 4233.
[31] M. P. Donzello, C. Ercolani, L. Mannina, E. Viola, A. Bubnova, O. Khelevina, P. A. Stuzhin, *Aust. J. Chem.* **2008**, *61*, 262.
[32] M. Kandaz, A. R. Özkaya, A. Koca, B. Salih, *Dyes Pigm.* **2007**, *74*, 483 – 489.
[33] J. W. Sibert, T. F. Baumann, D. J. Williams, A. J. White, A. G. M. Barrett, B. M. Hoffman, *J. Am. Chem. Soc.* **1996**, *118*, 10487 – 10493.
[34] C. F. Van Nostrum, F. B. Benneker, H. Brussaard, H. Kooijman, N. Veldman, A. L. Spek, J. Schoonman, M. C. Feiters, R. J. Nolte, *Inorg. Chem.* **1996**, *35*, 959 – 969.
[35] M. Durmuş, V. Ahsen, T. Nyokong, *J. Photochem. Photobiol. A* **2007**, *186*, 323 – 329.
[36] M. Gierszewski, M. Falkowski, L. Sobotta, M. Stolarska, L. Popenda, S. Lijewski, B. Wicher, G. Burdzinski, J. Karolczak, S. Jurga, M. Gdaniec, E. Tykarska, M. Sikorski, J. Mielcarek, T. Goslinski, *J. Photochem. Photobiol. A* **2015**, *307 – 308*, 54 – 67.
[37] I. Seotsanyana-Mokhosi, N. Kuznetsova, T. Nyokong, *J. Photochem. Photobiol. A* **2001**, *140*, 215 – 222.
[38] L. Sobotta, P. Fita, W. Szczolko, M. Wrotynski, M. Wierzchowski, T. Goslinski, J. Mielcarek, *J. Photochem. Photobiol. A* **2013**, *269*, 9 – 16.
[39] A. Ogunsipe, M. Durmuş, D. Atilla, A. G. Gürek, V. Ahsen, T. Nyokong, *Synt. Met.* **2008**, *158*, 839 – 847.
[40] A. Ogunsipe, D. Maree, T. Nyokong, *J. Mol. Struct.* **2003**, *650*, 131 – 140.
[41] J. Piskorz, P. Skupin, S. Lijewski, M. Korpusiński, M. Sciepura, K. Konopka, S. Sobiak, T. Goslinski, J. Mielcarek, *J. Fluorine Chem.* **2012**, *135*, 265 – 271.
[42] T. Goslinski, T. Osmalek, K. Konopka, M. Wierzchowski, P. Fita, J. Mielcarek, *Polyhedron* **2011**, *30*, 1538 – 1546.
[43] M. Wierzchowski, L. Sobotta, P. Skupin-Mrugalska, J. Kruk, W. Jusiak, M. Yee, K. Konopka, N. Düzgüneş, E. Tykarska, M. Gdaniec, J. Mielcarek, T. Goslinski, *J. Inorg. Biochem.* **2013**, *127*, 62 – 72.
[44] A. P. Thomas, P. S. Saneesh Babu, S. Asha Nair, S. Ramakrishnan, D. Ramaiah, T. K. Chandrashekar, A. Srinivasan, M. Radhakrishna Pillai, *J. Med. Chem.* **2012**, *55*, 5110 – 5120.
[45] S. Moon, J. Y. Bae, H. K. Son, D. Y. Lee, G. Park, H. You, H. Ko, Y. C. Kim, J. Kim, *Lasers Med. Sci.* **2015**, *30*, 499 – 507.
[46] Y. H. Moon, J. H. Park, S. A. Kim, J. B. Lee, S. G. Ahn, J. H. Yoon, *Head & Neck* **2010**, *32*, 1136 – 1142; Neck **2010**, 32, 1136 – 1142.
[47] S. H. Lim, C. Thivierge, P. Nowak-Sliwinska, J. Han, H. van den Bergh, G. Wagnières, K. Burgess, H. B. Lee, *J. Med. Chem.* **2010**, *53*, 2865 – 2874.
[48] S. S. Lucky, N. M. Idris, Z. Li, K. Huang, K. C. Soo, Y. Zhang, *ACS Nano* **2015**, *9*, 191 – 205.
[49] K. Matsumoto, M. Horikoshi, K. Rikimaru, S. Enomoto, *J. Oral Pathol. Med.* **1989**, *18*, 498 – 501.
[50] R. D. Fields, M. V. Lancaster, *Am. Biotechnol. Lab.* **1993**, *11*, 48 – 50.
[51] K. Konopka, E. Pretzer, P. L. Felgner, N. Düzgüneş, *Biochim. Biophys. Acta* **1996**, *1312*, 186 – 196.

Manuscript received: February 1, 2016
Accepted Article published: March 1, 2016
Final Article published: March 23, 2016